Carbohydrate Research 344 (2009) 1205–1212

Contents lists available at ScienceDirect

Carbohydrate Research

journal homepage: www.elsevier.com/locate/carres

Using pulse field gradient NMR diffusion measurements to define molecular size distributions in glycan preparations

Michelle C. Miller [a], Anatole Klyosov [b], David Platt [b], Kevin H. Mayo [a,*]

[a] Department of Biochemistry, Molecular Biology and Biophysics, University of Minnesota Health Sciences Center, 6-155 Jackson Hall, 321 Church Street, Minneapolis, MN 55455, United States
[b] Pro-Pharmaceuticals, Inc, 7 Wells Ave., Newton, MA 02459, United States

ARTICLE INFO

Article history:
Received 15 October 2008
Received in revised form 16 January 2009
Accepted 4 April 2009
Available online 17 April 2009

Keywords:
NMR
Diffusion
Carbohydrate
Glycan

ABSTRACT

Glycans comprise perhaps the largest biomass in nature, and more and more glycans are used in a number of applications, including those as pharmaceutical agents in the clinic. However, defining glycan molecular weight distributions during and after their preparation is not always straightforward. Here, we use pulse field gradient (PFG) ^{1}H NMR self-diffusion measurements to assess molecular weight distributions in various glycan preparations. Initially, we derived diffusion coefficients, D, on a series of dextrans with reported weight-average molecular weights from about 5 kDa to 150 kDa. For each dextran sample, we analyzed 15 diffusion decay curves, one from each of the 15 major ^{1}H resonance envelopes, to provide diffusion coefficients. By measuring D as a function of dextran concentration, we determined D at infinite dilution, D_{inf}, which allowed estimation of the hydrodynamic radius, R_h, using the Stokes–Einstein relationship. A plot of log D_{inf} versus log R_h was linear and provided a standard calibration curve from which R_h is estimated for other glycans. We then applied this methodology to investigate two other glycans, an α-(1→2)-L-rhamnosyl-α-(1→4)-D-galacturonosyl with quasi-randomly distributed, mostly terminal β(1→4)-linked galactose side-chains (GRG) and an α(1→6)-D-galacto-β(1→4)-D-mannan (Davanat), which is presently being tested against cancer in the clinic. Using the dextran-derived calibration curve, we find that average R_h values for GRG and Davanat are $76 \pm 6 \times 10^{-10}$ m and $56 \pm 3 \times 10^{-10}$ m, with GRG being more polydispersed than Davanat. Results from this study will be useful to investigators requiring knowledge of polysaccharide dispersity, needing to study polysaccharides under various solution conditions, or wanting to follow degradation of polysaccharides during production.

1. Introduction

Of the three major groups of biopolymers in nature (consisting of polynucleotides, polypeptides, and polysaccharides), polysaccharides are the most chemically and structurally diverse compounds.[1] For example, while polynucleotides and polypeptides only form linear polymers, polysaccharides can also form branched polymeric structures in various ways, with each glycosidic linkage making a new stereogenic center. Moreover, polysaccharides like their brethren can be phosphorylated, sulfated, methylated, acetylated, etc. In all, this makes the net of possible combinations and permutations much greater than that of polynucleotides and polypeptides. It is in fact their overall heterogeneity, combined with their ability to randomly self-associate, that has impeded their study and structural characterization.

Various biophysical approaches have been used to characterize and to understand physicochemical properties of polysaccharides in solution. Given that the molecular structures of large glycans cannot be determined to high resolution, that is, by X-ray and NMR, these have usually been investigated in terms of their hydrodynamic behavior in solution by measuring viscosity and diffusion properties to provide information, for example, on their solvent and intermolecular interactions, size, and overall shape. Ultracentrifugation and light scattering have been the primary methods normally used in these endeavors, for example, on glycogen,[2] hyaluronate,[3] carrageenans,[4] and chitosans.[5] Small angle X-ray scattering has been used as well, for example, on heparin,[6] as have rheological techniques, for example, with starch under various solution conditions to assess viscosities and derive interaction energies for structural insight.[7] Other novel approaches use size-exclusion chromatography and multi-angle laser light scattering (SEC-MALLS) for molecular weight determination of galactomann-

Abbreviations: NMR, nuclear magnetic resonance; PFG, pulse field gradient; GRG, galactorhamnogalacturonate glycan; DAVANAT, a galactomannan glycan, is trademarked.

* Corresponding author.
E-mail address: mayox001@umn.edu (K.H. Mayo).

0008-6215/$ - see front matter © 2009 Elsevier Ltd. All rights reserved.
doi:10.1016/j.carres.2009.04.010

ans,[8,9] and confocal fluorescence recovery after photobleaching (FRAP) to study diffusion and macromolecular organization of network forming FITC-labeled aggrecan, a high molecular weight proteoglycan containing chondroitin sulfate and keratin sulfate chains,[10] as well as to study the diffusion of FITC-labeled dextrans.[11] Still another versatile technique is pulse field gradient (PFG) NMR, which relies on variations in the strength of the applied magnetic field to dephase resonances depending on their diffusion properties, for example, with solutions and/or gels of hyaluronate[12,13] and dextran.[14,15] The PFG NMR technique is quite versatile and can be used with solutions, for example, at various pH values, ionic strengths, and temperatures, as well as with pre-gel solutions transitioning into gel states.

In the present study, we used the PFG NMR diffusion approach to derive translational diffusion coefficients for three polysaccharides: dextran, GRG, and Davanat. We first investigated five weight-average molecular weight (M_w) fractions of dextran with reported weight-average molecular weights of about 5, 24, 49, 81, and 148 kDa. For each fraction, we derived diffusion coefficients, D, as a function of the glycan concentration and determined D at infinite dilution, D_{inf}. Plots of log D_{inf} versus log M_w for the dextrans and lactose are linear, and a plot of log D_{inf} versus log of the hydrodynamic radius, R_h, calculated using the Stokes-Einstein relationship provides a standard correlation plot from which D values of other glycans may be related to the distribution of molecular sizes. We exemplify this approach here using the glycans GRG and Davanat, whose repeating motifs, along with that for dextran, are illustrated in Figure 1. The motif for GRG is mainly conjectural, as rhamnogalacturonans have irregular structures that have yet to be determined completely.[16–20]

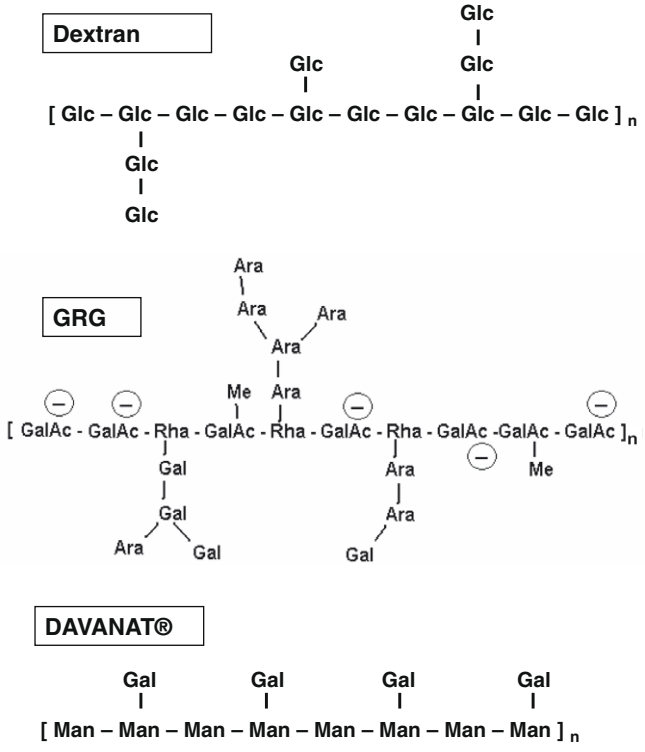

Figure 1. The chemical motifs for repeat units in dextran, GRG, and Davanat are shown. That for GRG is conjectural, and can hardly be considered a 'repeating' unit; rather, it represents a unit that can vary along the polysaccharide chain. The 3-letter code for saccharide units is used, where Glc, Gal, Man, Ara, Rha, GalAc stand for glucose, galactose, mannose, arabanose, rhamanose, and galacturonate, respectively. The 'Me' stands for methyl, as some of the carboxylate groups in galacturonate units can be methylated.

Davanat, isolated from Guar gum (*Cyamopsis tetragonoloba*) and subjected to a controlled partial depolymerization,[8] is a galactomannan whose backbone is composed of (1→4)-linked β-D-mannopyranosyl units to which single α-D-galactopyranosyl residues are attached via a (1→6)-linkage, with an average repeating unit of 17 β-D-Man residues and ten α-D-Gal residues, and an average polymeric molecule containing approximately 12 such repeating units. Thus the ratio of mannose to galactose in this compound is 1.7. GRG, produced from crude citrus pectins, is a galacto-rhamnogalacturonate of irregular structure, with a backbone composed mainly of α-(1→2)-L-rhamnosyl-α-(1→4)-D-galacturonosyl, with quasi-randomly distributed β-(1→4)-linked galactose side-chains, mostly at terminal positions. Both GRG and Davanat have been produced by controlled partial depolymerization of considerably larger polysaccharides (up to several million Daltons),[8,21] and as such it is important to know their size distributions.

2. Experimental

2.1. Glycan preparation

The isolation and purification procedure for Davanat when starting from a commercial *Cyamopsis tetragonoloba* guar gum flour, was used essentially as previously reported.[8] Briefly, the procedure has five principal steps: (1) aqueous extraction of galactomannans, (2) controlled partial depolymerization, (3) recovery as an insoluble copper complex, (4) recovery from the copper complex, and (5) repeated ethanol precipitations. The final yield of Davanat was typically 50% by weight of guar gum flour. The purification procedure results in a pure Davanat as a white powder with a solubility in water of more than 60 mg/mL, and a mannose:galactose ratio of 1.7. ^{1}H NMR and ^{13}C NMR spectra of Davanat are described by Platt et al.[8]

For GRG, the size reduction protocol uses controlled conditions (temperature, reaction time, and catalysts) with hydrogen peroxide and L-ascorbate to catalytically hydrolyze glycosidic linkages in the polysaccharide backbone and oligosaccharide side chains into smaller polysaccharide molecules (US Patent pending). This chemical modification is aimed at limited depolymerization of the backbone of the polymer, mainly the α-(1→2)-L-rhamnosyl-α-(1→4)-D-galacturonosyl sections, accompanied by de-methoxylation and de-acetylation of carboxylic groups of the polymer, which also decreases hydrophobicity, and hence increases aqueous solubility. Briefly, the crude commercially available citrus pectin is provided as solid crude powder, typically used in food industry, and is dissolved in distilled water to pH 10 with 3 M NaOH. After incubation at 50 °C for 30 min, 20% ethanol is added and the partially purified polysaccharide is precipitated to remove proteins and pigments. The polysaccharide is then dissolved to 20 g/L in water, followed by addition of trifluoroacetic acid to a final concentration of 0.5 M for controlled de-polymerization, which cleaves the galacto-rhamnogalacturonans backbone to the desired size. After incubation for 24 h at 60 °C, the solution pH is adjusted to 4, cooled to 4 °C, and centrifuged to remove insoluble matter. The supernatant is then neutralized to a final pH of 8.0 with 1 M NaOH, and 20% ethanol is added to recover soluble polysaccharide. The resulting soluble branched polysaccharide product (GRG) is washed with 70% ethanol or with 100% acetone to provide a final dry powder. Both Davanat and GRG were reduced in molecular weight compared to their starting materials in order to increase solubility and expose galactose residues for potentially better interactions with Gal-1.

A series of dextran samples of weight-average molecular weights of 5.2, 23.8, 48.6, 80.9, and 147.6 kDa were purchased from

Sigma–Aldrich and were used as received without further purification. For these dextran preparations, the manufacturer gives peak molecular weights and number-average molecular weights as 4.4, 21.4, 43.5, 66.7, 123.6 kDa, and 3.3, 18.3, 35.6, 55.5, 100.3 kDa, respectively. These values were derived using gel permeation chromatography. Throughout this text, we refer to these dextrans using their weight-average molecular weights, rounded to the nearest whole integer value.

2.2. Pulse field gradient NMR self-diffusion measurements

For NMR measurements, compounds were dissolved in 0.6 mL of unbuffered D_2O, and the pH was adjusted by adding microliter quantities of NaOD or DCl.

Pulse field gradient (PFG) NMR self-diffusion measurements were made on a Varian INOVA-600 using a GRASP gradient unit, as previously described.[22,23] NMR spectra for measurement of diffusion coefficients, D, were acquired using a 5 mm triple-resonance probe equipped with an actively shielded z-gradient coil. The maximum magnitude of the gradient was calibrated using the manufacturer's standard procedure based on the frequency spread of the applied gradient and was found to be 75 G/cm, which was consistent with the value obtained from analysis of PFG data on water using its known diffusion constant.[24] The linearity of the gradient was checked by performing diffusion measurements on water over different ranges of the gradient. The PFG longitudinal eddy-current delay pulse-sequence was used for self-diffusion measurements.[25] All NMR experiments were carried out at 30 °C. Raw data were converted and processed by using NMRPipe[26] and were analyzed by using NMRview.[27]

For unrestricted diffusion of a molecule in an isotropic liquid, the PFG NMR signal amplitude, A, normalized to the signal obtained in the absence of gradient pulses, is related to D by

$$A = \exp[-\gamma^2 g^2 \Delta^2 D(\Delta - \delta/3)] \quad (1)$$

where γ is the gyromagnetic ratio of the observed nucleus; g and δ are the magnitude and duration of the magnetic field gradient pulses, respectively, and Δ is the time between the gradient pulses.[28] For these experiments, $\delta = 3$ ms, $g = 1$–75 G/cm, $\Delta = 58.6$ ms, and the longitudinal eddy-current delay $T_e = 100$ ms. Each diffusion constant, D, was determined from a series of 12 one-dimensional PFG spectra acquired using different g values. Diffusion coefficient measurements were calibrated by performing the PFG NMR self-diffusion measurements on standard dextran samples having weight-average molecular weights of 5, 24, 49, 81, and 148 kDa.

3. Results and discussion

3.1. PFG NMR self-diffusion measurement of a series of dextrans

We first investigated a series of dextrans, with reported weight-average molecular weights of 5, 24, 49, 81, and 148 kDa, as well as the disaccharide lactose (0.36 kDa), and performed NMR pulse field gradient diffusion measurements as a function of the glycan concentration. A ^{1}H NMR spectral trace for the 81 kDa dextran sample (6.3 mg/mL) is shown in Figure 2. Resonances are labeled according to ^{1}H NMR assignments previously reported.[29] Even though these dextran samples comprise glycans of various molecular sizes and have monomer saccharide units in different structural positions (e.g., terminal, backbone, and side-chain), their NMR spectra are essentially the same because the chemical environment of any given monomer saccharide unit is not that different from any other. Nevertheless, PFG-induced dephasing at a given resonance position

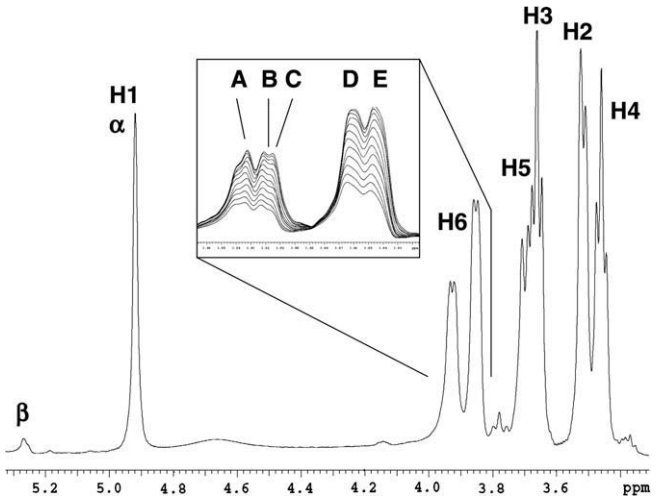

Figure 2. ^{1}H NMR spectrum of weight-average 81 kDa dextran sample is shown. The inset shows an exemplary set of stacked plots of NMR diffusion-mediated differentially dephased spectra of this dextran's H6 resonances. Peak positions used to derive diffusion decay curves shown in Figure 3A are labeled A–E. The most intense resonances occur at the start of the measurement when the gradient strength is weakest, and progressively decrease in intensity as gradient strength is increased and resonances become more dephased. Gradient strength is defined by Eq. 1, where $\delta = 3$ ms, $g = 1$–75 G/cm, and $\Delta = 58.6$ ms.

is quite sensitive to the presence of different size molecular species. The inset in Figure 2 exemplifies this by showing the differential gradient-induced dephasing at 5 positions (A–E) within the H6 resonance envelope of the 81 kDa dextran sample. Resonance intensities are a function of the gradient strength as defined by Eq. 1 (see Section 2), with the most intense resonance occurring at the start of the measurement when the gradient strength is weakest. As the gradient strength is increased, resonances become more dephased and therefore they decrease in intensity. More importantly, note that dephasing (intensity decrease) is not the same at all positions through the H-6 resonance envelopes, which it would be if there were only one molecular size species present.

This is more evident in Figure 3A which plots the logarithm of the fractional change in intensity of A–E (intensity divided by the initial intensity at zero gradient) versus gradient strength. Slopes of the resulting decay curves which effectively yield diffusion coefficients, D (see Eq. 1, Section 2), vary significantly for A–E. If we simply fit these data points with a straight line, we find that D values range from 0.32×10^{-6} cm^2/s (A), 0.35×10^{-6} cm^2/s (B), 0.47×10^{-6} cm^2/s (C), 0.28×10^{-6} cm^2/s (D), to 0.43×10^{-6} cm^2/s (E). These differences reflect differences in molecular sizes within this dextran sample. Moreover, some of the decay curves (i.e., B, C, and E) are non-linear, also indicating the presence of more than one molecular weight species at that particular chemical shift position (i.e., A–E). Because of this, we analyze decay curves from a number of resonances in each sample to provide a reasonable range of D values that we can then relate to molecular size.

When decay curves are curvi-linear, we can estimate the extrema of D values from a given decay curve by assessing the slope of initial and final groups of points on the curve. For example, the dashed line through the final 8 points on decay curve C in Figure 3A illustrates this for the 'slow' component of the full decay curve, whereas the initial four points define the 'fast' decay component. In this instance, we have D values of 0.6×10^{-6} cm^2/s for the fast component and of 0.44×10^{-6} cm^2/s for the slow component. Given that we are nearly at the limitation of gradient strength for our spectrometer, additional points on the decay curves could not be acquired. Nevertheless, D values derived from the slow component provide good and reasonable values, as linear fits using the final 8 data points yield R^2 values greater than 0.9. In addition, we

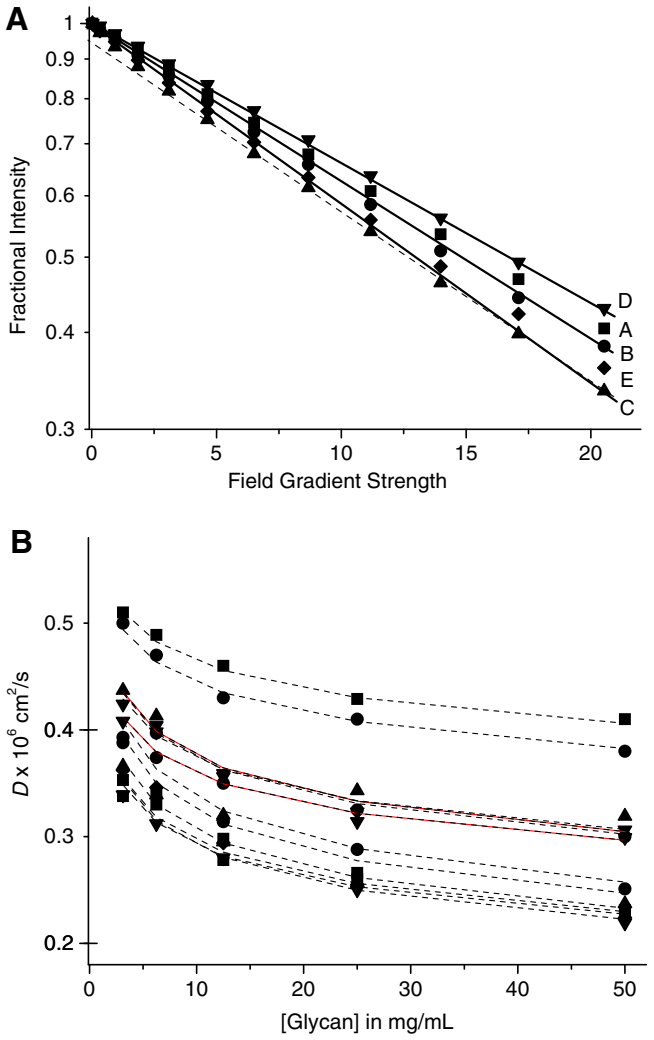

Figure 3. (**A**) For resonances A–E indicated in the inset in Figure 2, diffusion decay curves are shown as the logarithm of the change in intensity versus gradient strength. The slope effectively yields D_{obs} as defined in the text. Note that some of the decay curves are nonlinear, indicating a distribution (2 or more) of D values under that particular resonance. (**B**) Using a series of dextrans with reported weight-average molecular weights of 5, 24, 49, 81, and 148 kDa, as well as the disaccharide lactose (0.36 kDa), NMR pulse field gradient self-diffusion measurements were performed as a function of the glycan concentration. Plots of D_{obs} versus concentration of the 81 kDa dextran (mg/mL) are shown, which are used to estimate D values at infinite dilution, D_{inf}, by extrapolating D_{obs} to zero glycan concentration (Y-intercept) using a fitted curve as described in the text.

can estimate the fraction of the slow component by extrapolating the line for the slow component to the *Y*-intercept. In this case, the *Y*-intercept is −0.05, indicating that the slow component accounts for 89% (i.e., $10^{-0.05} \times 100$) of decay curve C. In other words, under point C in the NMR spectrum (Fig. 2), we have one major fraction (89%) of dextran represented. If there were only two components to the decay curve, then the fast component would account for the difference, or 11% of the decay curve. Although the estimate for the slow component is reliable, that for the fast component is only a crude estimate, because we do not know how many molecular weight fractions actually comprise each resonance. Nonetheless, the limits or extrema of these D values are good, reasonable estimates, and assessing fractional composition can be advantageous.

3.2. Correlation of self-diffusion of dextrans with their molecular sizes

In order to correlate D values of these dextran polymers with their molecular sizes, we determined D values as a function of dextran concentration, and extrapolated D to infinite dilution, yielding D_{inf}. For each dextran sample, we measured decay curves for the 15 most intense resonances. For example, for the 49 kDa dextran sample, D values were derived and are plotted as D versus concentration (mg/mL) in Figure 3B. Nonlinear decay curves were deconvoluted to yield fast and slow decay components as discussed above. However, only D values from the slow components were used in the following analysis, primarily because contributions from fast components were only about 10% of the decay curve, making determination of these D values less accurate.

Polysaccharides generally interact with each other to form networks in solution, and D values are quite sensitive to these intermolecular interactions which contribute significantly to solution viscosity. D is related to the viscosity-average molecular weight of the polymer, M_v, through the Mark–Houwink relationship, by the following equation which has been derived in its simplest form for a spherical particle:[30]

$$D = [RT/6\pi\eta_o N_o][10\pi N_o/3KM_v^{\alpha+1}]^{1/3} \quad (2)$$

where R is the gas constant, T is temperature in Kelvin, η_o is the viscosity of the liquid medium, N_o is Avogadro's number, and K ($cm^3\ g^{-1}$) and α are Mark–Houwink constants determined experimentally over a range of molecular weights and polymeric structures. For example, α is zero for a hard sphere, 2 for a rigid rod, 1 for a semi-coil, 0.5 in a Flory theta solvent, and 0.8 in a thermodynamically good solvent. For our purpose, we need only to consider that $D \propto [1/M_v^{\alpha+1}]^{1/3}$, and although this proportionality is truly valid only for a sphere, we can generalize it to $D \propto 1/M_v^b$. M_v is the viscosity-average molecular weight, and 'b' is some power to which M_v is raised. In this regard, the function has the phenomenological form:

$$y = a(1/x^b) \quad (3)$$

where 'a' and 'b' are fitting parameters, and we used this equation to fit our D versus concentration (mg/ml) curves in Figure 3B and derive D_{inf} from the *Y*-intercept. The fits shown in Figure 3B as dashed lines represent the data quite well, with D_{inf} values ranging from 0.42×10^{-6} cm^2/s to 0.58×10^{-6} cm^2/s for this '49 kDa' dextran sample. It should be noted that we derive essentially the same results by plotting $\log D_{obs}$ versus concentration in mg/mL and extrapolating to the *Y*-intercept at zero concentration.

On all five dextran samples, we determined D_{inf} for the 15 major resonances from each sample. Figure 4A plots $\log D_{inf}$ as a function of the log weight-average molecular weight as provided by the manufacturer. As should be evident from the above, there are multiple values for D_{inf} at any one given average molecular weight due to dextran size heterogeneity within each sample. Around each group of D_{inf} values, we drew a rectangle whose base indicates the molecular weight range provided by the manufacturer for each dextran sample. If the correlation between these D_{inf} values and the reported weight-average molecular weight range were perfect, we would be able to draw a straight line through the diagonals of each of these rectangles. Deviations result from our analysis not capturing all possible D values in each dextran sample and/or from the manufacturer's reported weight-average molecular weight distributions being somewhat off. Nevertheless, the apparent correlation (i.e., straight line) is rather good. In fact, the D value for the 0.36 kDa disaccharide lactose (5.5×10^{-6} cm^2/s, not shown in the plot) also lies on this straight line.

For a number of flexible polymers, Schmidt and Burchard[31] demonstrated that plots of D versus weight-average molecular

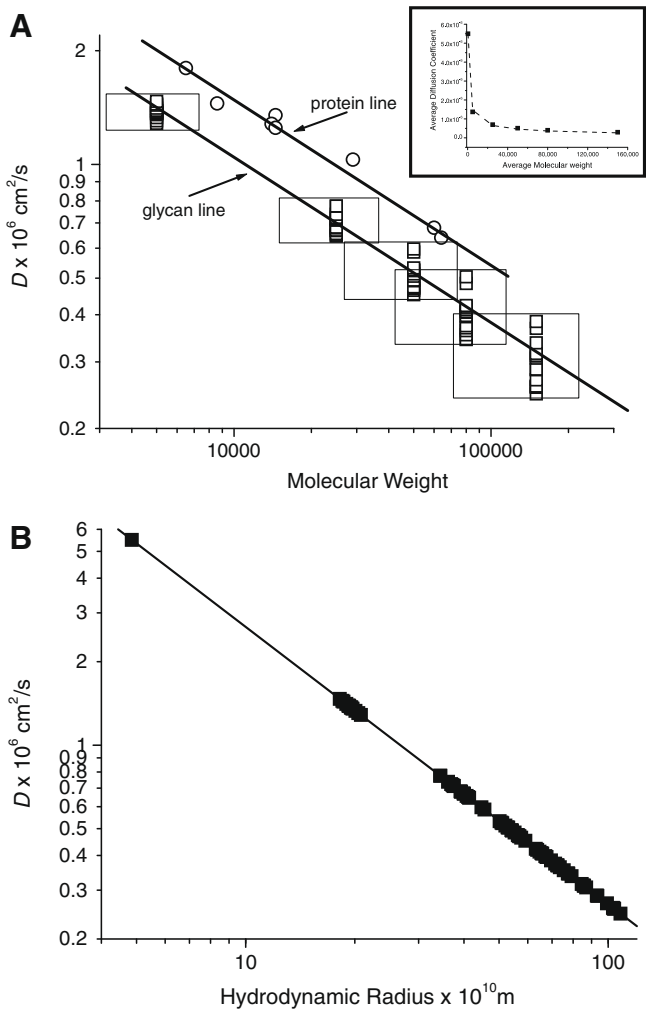

Figure 4. Calibration curves with standard dextrans. (**A**) log D_{inf} versus the log weight-average molecular weight provided by the manufacturer (see Section 2). Multiple values for D_{inf} at any given average molecular weight are observed due to the molecular weight distribution within each glycan sample. Around each group of D_{inf} values, a rectangle has been drawn, where its base is the mass range reported by the manufacturer for each glycan preparation. A straight line has been drawn through these points to represent the relationship between D_{inf} and weight-average molecular weight. A parallel straight line is also shown, with D values for standard proteins BSA (66 kDa), lysozyme (14.3 kDa), ribonuclease (13.6 kDa), and ubiquitin (8.6 kDa),[23] as well as for gal-1 monomer and dimer (Nesmelova et al., unpublished data). The inset in Figure 4A, which plots the average of these diffusion coefficients versus the average molecular weight, has been fit with a curve as described in the text. (**B**) log D_{inf} values for these dextrans, as well as for the disaccharide lactose, are plotted versus log hydrodynamic radius, R_h, calculated using the Stokes–Einstein relationship as discussed in the text. The linear fit shown has a regression coefficient $R^2 = 0.99$.

weight (M_w) follow a power law relationship having the form $D = \alpha(M_w)^{\beta}$. The inset in Figure 4A shows a nonlinear least squares fit ($R^2 > 0.99$) to our data using this equation, resulting in $\alpha = 11 \times 10^{-5}$ and $\beta = -0.5$. These values are similar to others that have been reported in the literature for various dextran solutions. A few examples are $\alpha = 5.5 \times 10^{-5}$ and $\beta = -0.43$ for dilute solutions of 20 kDa to 2000 kDa dextran,[32] and $\alpha = 2.7 \times 10^{-5}$ and $\beta = -0.37$ using a fluorescence photobleaching technique on solutions of 20 kDa to 2000 kDa FITC-labeled dextran samples.[10] The FITC-labeling fluorescence approach used solutions of dextran in the concentration range of 0.0125–0.2 mg/mL, whereas we are using dextran concentrations in the 3–50 mg/mL range. While differences in α and β fitting parameters among these studies may be explained in part by differences in dextran concentrations, it may also be explained by differences in branching or polydispersity of dextran samples.

The D_{inf} versus M_w plot (Fig. 4A) also reflects the random coil nature of these polysaccharides. The Stokes–Einstein equation $D = k_B T/6\pi\eta R_h$ relates D to the macromolecular hydrodynamic radius, R_h, which in turn is generally accepted as being proportional to a power, x, of the apparent molecular weight, M_{app}. This relationship can be used to compare D values for two molecules (Eq. 4) under the same solution conditions:

$$D_1/D_2 = (M_{2app}/M_{1app})^x \quad (4)$$

Typically, $x = 1/3$ for a compactly folded molecule, and $x = 1/2$ for a random coil state.[33] Because the Stokes–Einstein relationship has been derived specifically for a hard sphere, the actual molecular shape and the shape of the molecular aggregate will affect D, but usually only by about 10% when comparing two molecules having equal total volumes.[34] By using Eq. 4, D_{inf} values for our glycan standards versus their molecular weights (Fig. 4A) can be approximated with $x = 1/2$, indicating that these glycans, as expected, are random coil polymers.

For comparison, Figure 4A also plots D values for several globular proteins (6 kDa BPTI, 8.6 kDa ubiquitin, 13.6 kDa ribonuclease, 14.5 kDa galectin-1 monomer and its dimer form, 14.3 kDa lysozyme, 66 kDa BSA, and 64 kDa hemoglobin), as reported earlier by Ilyina et al.[23] As a function of molecular weight, these protein D values also follow a linear relationship, which parallels that for the dextrans, but is better approximated in Eq. 4 with $x = 1/3$, as expected for a well folded, globular structure. The shift in the protein line to a higher D value for any given molecular weight is likely explained by the random coil nature of these glycans, as well as by their inter-molecular (glycan–glycan) and solvent water interactions, compared to proteins.

Even though the plot of D versus M_w in Figure 4A is fine when comparing highly similar glycans, for example, our series of dextrans, it only yields apparent molecular weights, not true molecular weights, it could be misleading when using it to derive M_w from D values of other glycans, as is well known from size-exclusion chromatography (SEC) studies.[35] In fact, with both SEC and PFG NMR measurements, the relevant quantity to differentiate diffusion properties is physical size or hydrodynamic volume of a polymer chain and not molecular weight, primarily because a polymer chain can have different molecular weights, yet the same size due to differences in, for example, chemical nature, branching, flexibility, and solvation.[36,37] Nevertheless, it is interesting that simple lactose, which has no supermolecular or highly hydrated glycan structure, also falls on the linear curve of D_{inf} versus M_w (Fig. 4A), suggesting that perhaps diffusion coefficients derived from PFG NMR experiments may provide for meaningful weight-average molecular weights when comparing different glycan species. In any event, a more reliable calibration curve relates D to the hydrodynamic radius, R_h, when comparing chemically and structurally different glycans. In this regard, Figure 4B plots D_{inf} for these dextrans versus R_h calculated using the Stokes–Einstein relationship ($D = k_B T/6\pi\eta R_h$) with the solution viscosity η at $T = 303$ K being taken as 0.83×10^{-3} N s/m^2 for water at infinite dilution of solute. The data points, which include D for the disaccharide lactose, are fit well with a linear curve ($R^2 = 0.99$).

3.3. Size distributions of DAVANAT and GRG

We next used the PFG NMR diffusion method to investigate molecular size distributions in samples of two different glycans: GRG and Davanat. Even though GRG and Davanat are polysaccharides like dextran, they are structurally different from dextran and from each other. GRG is a highly branched, galactorhamnoga-

lacturonate of irregular structure, with a backbone that is composed primarily of α-(1→2)-L-rhamnosyl-α-(1→4)-D-galacturonosyl sections, and the weight-average molecular weight and molecular size distribution of this GRG preparation are unknown. The galactomannan Davanat has a 17 β(1→4)-D-mannopyranosyl/10 α-(1→6)-D-galactopyranosyl residue repeat fragment (Fig. 1), with reports of its M_w being 48–55 kDa.[8] Both GRG and Davanat have been prepared by controlled partial depolymerization, as explained in Section 2.

^{1}H NMR spectra of both polysaccharides are shown in Figure 5A (GRG) and 5B (Davanat). The more diverse and seemingly complex ^{1}H NMR spectrum of GRG is consistent with the presence of more varied types of saccharide units within its polymeric structure, compared to Davanat whose ^{1}H NMR spectrum is more similar to

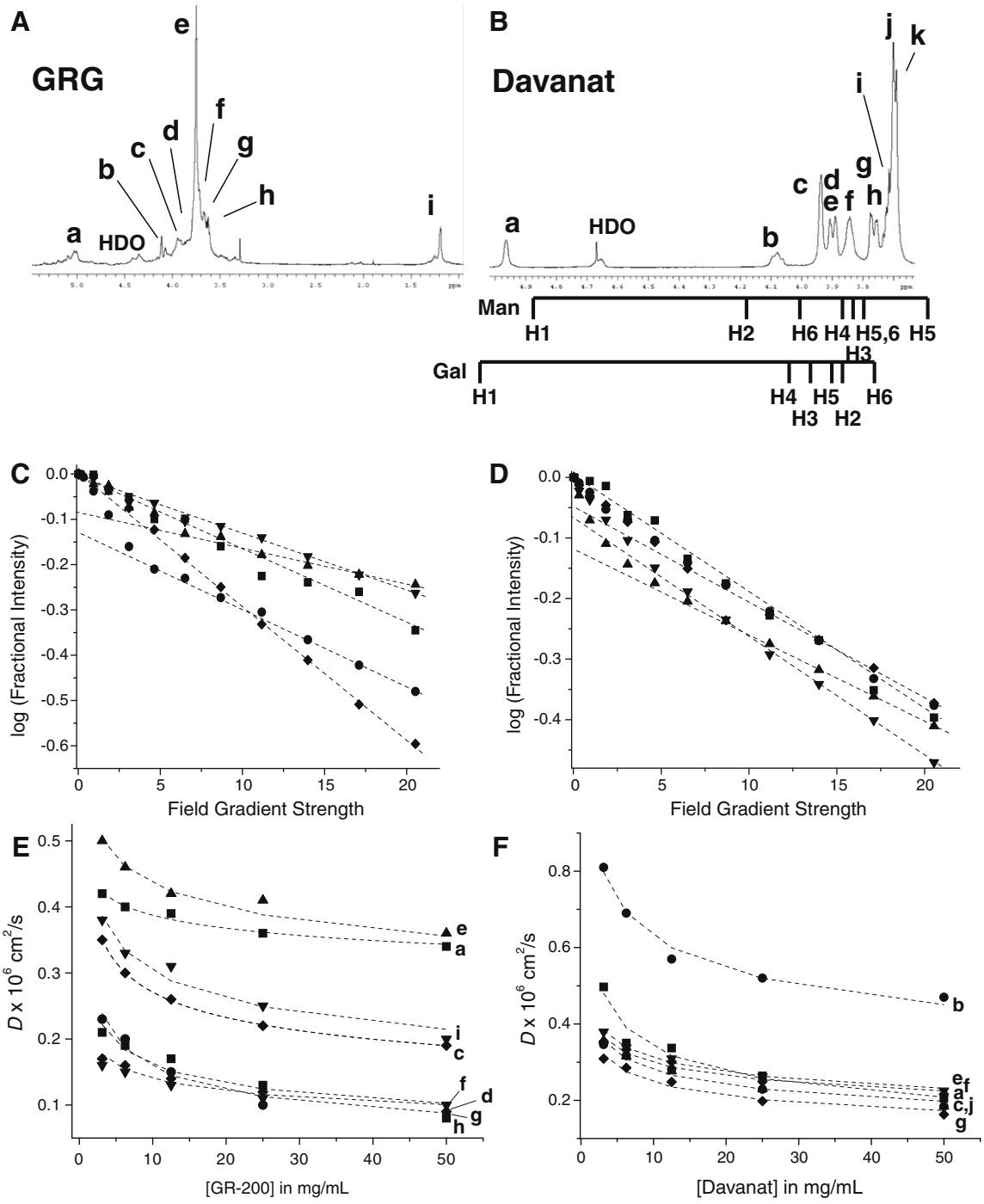

Figure 5. ^{1}H NMR spectral traces for GRG (**A**) and Davanat (**B**) are shown, and resonances are labeled alphabetically, with letters corresponding to curves shown in the plots shown below these spectra, and with D_{inf} values given in Table 1. Sets of diffusion decay curves are plotted as the log of the change in resonance intensity versus gradient strength for GRG (**C**) and Davanat (**D**). The slope effectively yields D as discussed in the text. Note that some of the decay curves are nonlinear, indicating a distribution (two or more) of D values under that particular resonance. Dashed lines are drawn through the slow components of these decay curves, as discussed in the text. D_{obs} values are plotted versus concentration (mg/mL) for GRG (**E**) and Davanat (**F**). As discussed in text, dashed lines represent fits of the data to the equation $y = a(1/x^b)$ to D_{inf} from the Y-intercept. ^{1}H resonance assignments for another galactomannan reported by Rakhmanberdyeva and Shashkov (2005) have been given under the spectrum of Davanat. Man (1→4 and 1→6 Gal-linked) and Gal stand for mannose and galactose units.

that of dextran. Resonance assignments for preparations of galactomannans from *Gleditsia delavayi* and *G. aquatica* have been reported by Rakhmanberdyeva and Shashkov.[38] However, because Davanat is a highly processed galactomannan, these assignments do not correspond exactly and unambiguously with chemical shifts of resonances in the ^{1}H spectrum of Davanat. Nevertheless, we have indicated them under the Davanat spectrum (Fig. 5B), for easy reference. Although unambiguous or specific assignments for ^{1}H resonances of GRG and DAVANAT are unknown, these are not really necessary for purposes of this study. Figure 5C and D gives several representative diffusion decay curves derived from gradient-induced dephasing of some resonances of GRG and Davanat, respectively. While some of these decay curves appear linear, most are at least somewhat curvi-linear, with slower decay components (indicated by dashed lines) usually dominating by 80–90%, as estimated from *Y*-intercepts. Curvi-linear decay curves indicate the presence of at least two (or more) significantly different sized glycans, whose resonances overlap at that chemical shift position.

Figure 5E and F plots D_{obs} versus concentration (mg/mL) for the major resonances from GRG and Davanat, respectively, as labeled alphabetically in their respective spectra in Figure 5A and B. Each set of data was fit using Eq. 2 as discussed above, and the dashed lines through the data points show the actual curve fits, with R^2 values being greater than 0.9. The *Y*-intercept provided estimates of *D* values at infinite dilution. For either glycan, D_{inf} values ranged from about 0.2×10^{-6} cm^2/s to 1.55×10^{-6} cm^2/s, and tended to be expectedly smaller for the larger GRG. These values are listed out in Table 1 for all or most of the resonances shown in the ^{1}H spectra of Figure 5.

Using these D_{inf} values, we estimated both R_h and weight-average molecular weights (M_w) using the dextran calibration curves (Fig. 4) as listed out in Table 1. For GRG, although R_h ranges from 17×10^{-10} m to 134×10^{-10} m, most values fall in the range of 46×10^{-10} m to 92×10^{-10} m, with a simple average of $76 \pm 6 \times 10^{-10}$ m. For the smaller Davanat glycan, the range of R_h is much narrower with a simple average of $56 \pm 3 \times 10^{-10}$ m, and most values falling in the range of 53×10^{-10} to 67×10^{-10} m. If we assume that GRG and Davanat behave similarly in solution as the dextrans, we find that weight-average molecular weight (M_w) values estimated from Figure 4A range from 3 kDa to 300 kDa for GRG and from 10 kDa to 80 kDa for Davanat, with simple average values of 128 ± 35 kDa and 59 ± 8 kDa, respectively (Table 1). Table 1 also provides estimates of the fractional contribution from each resonance derived by integrating resonances in the NMR spectra of each glycan. The average values given in parentheses were determined using these fractions as weighting factors. In either case, average values determined either way are nearly the same.

Although we have no values in the literature with which to compare our values for GRG, we do for Davanat, at least in terms of the weight-average molecular weight. Our weight-average molecular weight for Davanat (59 kDa) compares favorably with values reported previously (48–55 kDa) using the SEC-MALLS technique.[8] Using the PFG NMR diffusion approach, however, we also now have information on how dispersed these glycan preparations are. Clearly, GRG is more highly poly-dispersed than Davanat, which is expected based on the chemistry of these polysaccharides.

In summary, we have shown that PFG NMR is a useful approach to assess diffusion coefficients and to estimate molecular weights of various glycans without the need to have highly fractionated samples. The PFG NMR technique can be used with solutions, for example, at various pH values, ionic strengths, and temperatures, as well as with pre-gel solutions transitioning into gel states. As interest in carbohydrate research is increasing, this methodology should be quite useful to investigators needing to have knowledge of polysaccharide dispersity in solution, and to follow degradation of polysaccharides during chemical production.

Table 1
Diffusion coefficients for GRG and Davanat

Peak	Fraction	D_{inf}	R_h (10^{-10} m)	M_w (kDa)
GRG				
a	0.1	0.46 ± 0.01	58 ± 2	61 ± 5
b	0.03	1.55 ± 0.01	17 ± 1	3 ± 1
c	0.05	0.29 ± 0.01	92 ± 4	160 ± 15
d	0.15	0.2 ± 0.01	134 ± 7	300 ± 25
e	0.3	0.58 ± 0.07	46 ± 7	37 ± 10
f	0.08	0.22 ± 0.02	121 ± 12	270 ± 45
g	0.08	0.36 ± 0.04	74 ± 9	105 ± 25
h	0.08	0.3 ± 0.04	89 ± 14	160 ± 50
i	0.08	0.49 ± 0.03	55 ± 4	55 ± 7
Average			76 ± 6 (72)	128 ± 35 (118)
Davanat				
a	0.05	0.68 ± 0.06	39 ± 4	25 ± 5
b	0.1	1.0 ± 0.04	27 ± 2	10 ± 2
c	0.1	0.47 ± 0.02	57 ± 3	58 ± 7
d	0.05	0.4 ± 0.02	67 ± 4	85 ± 8
e	0.05	0.47 ± 0.01	57 ± 2	58 ± 5
f	0.15	0.45 ± 0.02	59 ± 3	65 ± 7
g	0.05	0.41 ± 0.02	65 ± 4	80 ± 9
h	0.05	0.43 ± 0.01	62 ± 2	73 ± 5
i	0.1	0.44 ± 0.03	61 ± 5	69 ± 9
j	0.2	0.42 ± 0.02	64 ± 4	76 ± 8
k	0.1	0.5 ± 0.02	53 ± 3	52 ± 7
Average			56 ± 3 (56)	59 ± 8 (60)

Diffusion coefficients (10^{-6} cm^2/s) at infinite dilution, D_{inf}, are given for NMR peaks identified in Figure 5. The fraction of each peak is based on spectral integration. The hydrodynamic radius, R_h (10^{-10} m), was calculated using the Stokes–Einstein relationship ($D_{inf} = k_B T/6\pi\eta R_h$) with $T = 303$ K, the Boltzman constant $k_B = 1.38 \times 10^{-23}$ N m/K, and the solution viscosity η for water (infinite dilution of solute) at 303 K, that is, 0.83×10^{-3} N s/m^2. Apparent weight-average molecular weights (M_w) were derived from the standard curve shown in Figure 3B. Simple average values of R_h and M_w listed are shown at the bottom of each respective column, and the average value in parentheses is calculated using the fraction from resonance peak intensities.

Acknowledgment

This work was sponsored by a research grant from the National Cancer Institute (NIH award R01 CA096090) to K.H.M. Michelle Miller is supported by the Cancer Biology Training Grant from the NIH (T32 CA009138). NMR instrumentation was provided with funds from the National Science Foundation (BIR-961477), the University of Minnesota Medical School, and the Minnesota Medical Foundation.

References

1. Werz, D. B.; Ranzinger, R.; Herget, S.; Adibekian, A.; von der Lieth, C.-W.; Seeberger, P. H. *Chem. Biol.* **2007**, *2*, 685–691.
2. Geddes, R.; Harvey, J. D.; Wills, P. R. *Biochem. J.* **1977**, *163*, 201–209.
3. Bartold, P. M.; Wiebkin, O. W.; Thonard, J. C. *Connect. Tissue Res.* **1984**, *12*, 257–264.
4. Slootmaekers, D.; Mandel, M.; Reynaers, H. *Int. J. Biol. Macromol.* **1991**, *13*, 17–25.
5. Errington, N.; Harding, S. E.; Varum, K. M.; Illum, L. *Int. J. Biol. Macromol.* **1993**, *15*, 113–117.
6. Pavlov, G.; Finet, S.; Tatarenko, K.; Korneeva, E.; Ebel, C. *Eur. Biophys. J.* **2003**, *32*, 437–449.
7. De Vasconcelos, C. L.; de Azevedo, F. G.; Pereira, M. R.; Fonseca, J. L. C. *Carbohydr. Polym.* **2000**, *41*, 181–184.
8. Platt, D.; Klyosov, A. A.; Zomer, E. In *Carbohydrate Drug Design,* Anatole, A. K.; Witczak, Z. J.; David, P. Eds.; ACS Symposium Series 932; American Chemical Society: 2006; pp 49–66.
9. Pollard, M. A.; Kelly, R.; Wahl, C.; Fischer, P.; Windhab, E.; Eder, B.; Amado, R. *Food Hydrocolloid* **2007**, *21*, 683–692.
10. Gribbon, P.; Hardingham, T. E. *Biophys. J.* **1998**, *75*, 1032–1039.
11. Mazza, D.; Braeckmans, K.; Cella, F.; Testa, I.; Vercauteren, D.; Demeester, J.; De Smedt, S.S.; Diaspro, A. *Biophys. J.* **2008** (July 11, 2008 epub).
12. Masuda, A.; Ushida, K.; Koshino, H.; Yamashita, K.; Kluge, T. *J. Am. Chem. Soc.* **2001**, *123*, 11468–11471.

13. Taglienti, A.; Valentini, M.; Sequi, P.; Crescenzi, V. *Biomacromolecules* **2005**, *6*, 1648–1653.
14. Naji, L.; Schiller, J.; Kaufmann, J.; Stallmach, F.; Kärger, J.; Arnold, K. *Biophys. Chem.* **2003**, *104*, 131.
15. Kwak, S.; Viet, M. T.; Lafleur, M. *J. Magn. Reson.* **2003**, *162*, 198–205.
16. Deng, C.; O'Neill, M. A.; York, W. S. *Carbohydr. Res.* **2006**, *341*, 474–484.
17. Willats, W. G.; McCartney, L.; Mackie, W.; Knox, J. P. *Plant Mol. Biol.* **2001**, *47*, 9–27.
18. Oomen, R. J. F. J.; Doeswijk-Voragen, C. H. L.; Â Bush, M. S.; Â Vincken, J-P.; Â Borkhardt, B.; Â van den Broek, L. A. M.; Â Corsar, J.; Â Ulvskov, P.; Â Voragen, A. G. J.; Â McCann, M. C.; Â Visser, R. G. F. *Plant J.* **2002**, *30*, 403–413.
19. Vidal, S.; Doco, T.; Williams, P.; Pellerin, P.; York, W. S.; O'Neill, M. A.; Glushka, J.; Darvill, A. G.; Albersheim, P. *Carbohydr. Res.* **2000**, *326*, 277–294.
20. Glushka, J. N.; Terrell, M.; York, W. S.; O'Neill, M. A.; Gucwa, A.; Darvill, A. G.; Albersheim, P.; Prestegard, J. H. *Carbohydr. Res.* **2003**, *13381*, 341–352.
21. Klyosov, A. A.; Platt, D.; Zomer, E. *Preclinica* **2003**, *1*, 175–186.
22. Mayo, K. H.; Ilyina, E.; Park, H. *Protein Sci.* **1996**, *5*, 1301–1315.
23. Ilyina, E.; Roongta, V.; Pan, H.; Woodward, C.; Mayo, K. H. *Biochemistry* **1997**, *36*, 3383–3388.
24. Mills, R. *J. Phys. Chem.* **1973**, *77*, 685–688.
25. Gibbs, S. J.; Johnson, C. S. *J. Magn. Reson.* **1991**, *93*, 395–402.
26. Delaglio, F.; Grzesiek, S.; Vuister, G. W.; Zhu, G.; Pfeifer, J.; Bax, A. *J. Biomol. NMR* **1995**, *6*, 277–293.
27. Johnson, B. A.; Blevins, R. A. *J. Biomol. NMR* **1994**, *4*, 603–614.
28. Stejskal, E. O.; Tanner, J. E. *J. Chem. Phys.* **1965**, *42*, 288–292.
29. Dinadayala, P.; Lemassu, A.; Granovski, P.; Cérantola, S.; Winter, N.; Daffé, M. *J. Biol. Chem.* **2004**, *279*, 12369–12378.
30. Rudin, A.; Johnston, H. K. *Polym. Lett.* **1971**, *9*, 55–60.
31. Schmidt, M.; Burchard, W. *Macromolecules* **1981**, *14*, 210–211.
32. Amu, T. C. *Biophys. Chem.* **1982**, *16*, 269–273.
33. Cantor, C. R.; Schimmel, P. R. *The behavior of Biological Macromolecules. Biophysical Chemistry*, Part III, W. H. Freeman, New York, 1980; pp 979–1039.
34. Teller, D. C.; Swanson, E.; de Haen, C. *Methods Enzymol.* **1979**, *61*, 103–124.
35. Guillaneuf, Y.; Castignolles, P. J. *Polym. Sci. A Polym. Chem.* **2008**, *46*, 897–911.
36. Couvreur, L.; Piteau, G.; Castignolles, P.; Tonge, M.; Coutin, B.; Charleux, B.; Vairon, J. P. *Macromol. Symp.* **2001**, *174*, 197–207.
37. Netopilik, M.; Kratochvil, P. *Polymer* **2003**, *44*, 3431–3436.
38. Rakhmanberdyeva, R. K.; Shashkov, A. S. *Chem. Nat. Compd.* **2005**, *41*, 14–16.